In vitro cellular response to oxidised collagen-PLLA hybrid scaffolds designed for the repair of muscular tissue defects and complex incisional hernias

Fanrong Pu[a]*, Nicholas P Rhodes[a], Yves Bayon[b] and John A Hunt[a]

[a] Clinical Engineering, Institute of Ageing and Chronic Disease, University of Liverpool, Duncan Building, Daulby Street, Liverpool L69 3GA, UK

[b] Covidien - Sofradim Production, 116 Avenue du Formans, 01600 Trevoux, France

* Corresponding author: Tel.: +44-151 706 4219
Fax: +44 151 706 4915

E-mail: frpu@liv.ac.uk

Abstract

Unique poly(L-lactic acid) (PLLA)-based scaffolds were constructed by embedding knitted PLLA yarns within a bioresorbable and differentially crosslinked three-dimensional (3D) oxidized collagen scaffold. The scaffolds were designed specifically for the repair of complex incisional abdominal wall hernias and the repair of defects within planar muscular tissues, such as the bladder. The chemical composition of the collagen matrix and the percentage of scaffold infiltration were compared for the different scaffold compositions. The results demonstrate that the incorporation of the collagen sponge within the PLLA scaffold facilitated bladder smooth muscle cell (bSMC) adhesion and proliferation. The highest dose of oxidized collagen (Oxicol) demonstrated better cell adhesion, resulting in the largest cell densities and most uniform distribution throughout the 3D collagen sponge. This formulation promoted the greatest α-smooth muscle actin (αSMA) expression detected through immunohistochemical staining and western blotting. For abdominal wall repair applications, the proliferation and differentiation of C2C12 myoblasts and myotube formation were studied. Following 7 days of myogenic induction, the greatest expression of mRNA of the myogenic markers myogenin and MRF4 was observed within the scaffolds with the highest dose of oxidized collagen, 1.5- and 3.85-fold greater expressions, respectively, compared to PLLA with unmodified collagen. Furthermore, in vitro myotube formation and MyMC expression were enhanced in the Oxicol scaffolds. We conclude that the Oxicol scaffold formulation with a high-dose oxidized collagen ratio provides enhanced myogenesis and αSMA, and the biological induction cues necessary to achieve better tissue integration, than standard PLLA scaffolds in the treatment of complex abdominal wall hernias.

Keywords: large complex abdominal wall defect; incisional hernia; tissue engineering; skeletal muscle; smooth muscle; PLLA; collagen; biodegradable polymers

1. Introduction

Of all patients who undergo any form of abdominal surgery, 11–20% suffer an incisional hernia (Mudge and Hughes, 1985; Santora and Roslyn, 1993; Sugerman *et al.*, 1996), where a weakness in the soft tissue results in postsurgical mechanical failure of the abdominal wall's integrity. This rises to approximately 20% of all bariatric surgeries (Hodgson et al., 2000; Luijendijk *et al.*, 2000; Cassar and Munro, 2002; Hoer *et al.*, 2002; Sorensen *et al.*, 2005; Kingsnorth, 2006; Millennium Research Group, 2009, 2010). Currently, 150 000 failures occur in the four largest markets in Europe (Millennium Research Group, 2009) and 350,000 cases are treated in the USA every year (Millennium Research Group, 2010). In each market there is a current growth rate of incidence of herniation of 3%/year, with an estimated>1 million patients/year, globally, requiring treatment. In obese patients, those with chronic renal disease, diabetics and those undergoing immunosuppressive or radiation therapy, acute wound-healing failure is most often the direct cause. The aetiology of the failure strongly suggests reduced blood flow and immunological factors, with high levels of bacterial contamination and necrosis at the site of herniation commonly observed (Leber *et al.*, 1998). No ideal surgical management procedure as yet exists, because repair surgery results in subsequent failure of the closure in a large proportion of incisional hernias, up to 54% in suture repairs and 36% in mesh repairs (Hodgson *et al.*, 2000; Burger *et al.*, 2004) requiring re-operation. Current technologies and changes to surgical practice have not improved the rate of incisional herniation over the past decade (Bellon, 2007) and only marginally over the past century (Carlson, 1997). The estimated annual cost of incisional hernia repair was $2.5 billion in the USA alone in 2001 (Arrow, 2001). Current procedures to repair ventral hernias can result in adhesions which may be extremely painful, often requiring further re-operation. Additional to these figures is the cost due to loss of economic activity and huge loss of quality of life in the affected patients.

Ventral hernias are termed 'complex' when: (a) they involve a surgical field that has been compromised due to tissue bacterial contamination; (b) the presence of gastrointestinal or biliary contents, due to a fistula or ostomy, loss of abdominal domain (presence of a large hernia sac) or dimensions that are >10 cm in any direction; (c) or are a re-operation of a contaminated mesh or re-opened ventral hernia. The repair of large, complex ventral hernias, which occur more commonly in obese patients, suffer exaggerated rates of bacterial contamination and necrosis. As the tissue immediately adjacent to the wound site is often exposed to enteric contents, it is very common for the closure of these hernias to fail (or fail again), leading to chronic repeat operations and, for obvious reasons, complete loss of quality

of life and economic output for the patient. Complex hernias often require extensive debridement of contaminated tissue around the hernia. Synthetic meshes are contra-indicated in the repair of these hernias (Blatnik *et al.*, 2008), due to the high rate of chronic contaminations that they subsequently harbour, due to low vascularization and tissue necrosis. However, autologous tissue is not often easily, surgically available in these patients. Acellular matrix grafts, such as allogeneic dermis grafts that have been decellularized and defatted from biological tissues, have demonstrated successful abdominal wall reconstruction and some resistance to bacterial contamination (Park *et al.*, 2006), but they are generally only slowly remodelled as a neotissue or are degraded too quickly (Valentin *et al.*, 2006).

There is an urgent need, therefore, for a biosynthetic alternative whose degradation properties can be tuned and which not only supports or enhances the growth and integration of abdominal wall cells and tissue, but which will allow or induce adequate levels of angiogenesis and vascularization. This will aid in prevention of necrosis and inhibition of chronic implant contamination.

In general, synthetic polymers have good mechanical strength, but they are relatively hydrophobic and hinder cell adhesion. Conversely, naturally derived polymers, such as collagen, contain a variety of cell adhesion domains whilst being hydrophilic. However, scaffolds constructed entirely from purified collagen fibres have generally demonstrated poor mechanical strength.

In this study, a novel design approach was taken by combining the advantageous biological properties of collagen with the strength of a synthetic PLLA scaffold, using a new chemical modification of collagen to modulate its degradation profile. A review of the literature has revealed that, until now, there have been no reports of collagen–PLLA composite materials for the repair of large complex abdominal wall defects. These considerations formed the motivation for the research described here.

Engineering skeletal muscle tissue for the repair of an abdominal wall defect requires the proliferation and differentiation of mononucleated muscle precursor cells (myoblasts) and their fusion into multinucleated myotubes, followed by the alignment of the myotubes into fibres (Wigmore and Dunglison, 1998). In this study, we used C2C12 myoblasts because they have been shown to faithfully mimic skeletal muscle differentiation *in vitro*, as shown by their induction to terminally differentiated myotubes following withdrawal of serum from the culture medium (Yaffe and Saxel, 1977; Pownall *et al.*, 2002; Parker *et al.*, 2003). Myogenic regulatory factors (MRFs) are skeletal muscle-specific transcription factors that are expressed during myogenic differentiation, the most important of which are MyoD, myogenin, Myf-5 and

MRF-4. Myf5 and MyoD are required for myoblast lineage specificity; myogenin is critical for the function of MRF-4 and differentiation; whilst myosin heavy chain II (MyHC) is expressed in fully differentiated fibres. In this study, we comprehensively studied the expression of myogenic regulator genes and proteins and determined whether the PLLA–collagen three-dimensional (3D) scaffolds were able to support myogenic differentiation and myotube formation.

αSMA is an important marker of functional bladder smooth muscle cells (bSMCs). We also investigated in the present study whether the PLLA–collagen scaffolds were able to sustain bSMC adherence, proliferation and continued expression of αSMA over an extended period, to determine whether the design was also appropriate for smooth muscle-containing regenerated tissue, such as tissue-engineered bladder. We also researched the best combination of PLLA–collagen 3D scaffolds for bladder applications by monitoring the expression of the SMC functional protein αSMA within the scaffold.

2. Materials and Methods

2.1. Preparation of collagen

Porcine collagen type I was extracted from porcine dermis by solubilization at acidic pH or by digestion with pepsin, and then purified by saline precipitation (Tinois *et al.*, 1991; Afanasiev *et al.*, 1999). Dry collagen fibres were obtained by precipitation of an acid solution of collagen by adding NaCl, then subsequent washing and drying of the precipitate, using increasing concentrations of acetone in the range 80–100%.

2.2. Glutaraldehyde (GTA)-crosslinking of collagen

Porcine collagen was crosslinked using glutaraldehyde (GTA) to inhibit complete. Collagen solution of 1% w/v concentration was neutralized using sodium phosphate at a final concentration of 20 mM, the resultant pH adjusted to be in the range 6.5–7.5. GTA (25% w/v; Fluka AG, Buchs, Switzerland) was added to the suspension at a final concentration of 0.5–0.8% w/v. Following 2 h incubation at ambient temperature, the collagen fibres were recovered by filtration of the suspension through a nylon mesh. The fibres were then treated with sodium borohydride for at least 2 h until the yellow colouration of the fibres had completely disappeared. The white fibres thus obtained were washed and neutralized at pH 6.5–7.5, and dried by removal of the water using acetone. The fibres were stored at -20°C following acetone removal by evaporation.

2.3. Chemical modification of collagen (fabrication of Oxicol)

The oxidation of porcine collagen (Oxicol formation) allows for its short-term remodelling when implanted in a host. Collagen was prepared by dissolving in 0.01 N HCl at a concentration of 30 g/l, then mixing with periodic acid to a final concentration of 8 mM. Oxidation was performed at an ambient temperature close to 22°C for 3 h in the dark. An equal volume of a solution of sodium chloride was added to obtain a final concentration of 41 g/l NaCl. The precipitate was collected after 30 min by decantating through a fabric filter (porosity of 100 μm), then washing four times with a 41 g/l solution of NaCl in 0.01 N HCl to form an acid saline precipitate. This washing process eliminated all traces of periodic acid and iodine derivatives formed during oxidation of the collagen. The collagen precipitate was washed several times in an aqueous solution of 80% acetone to eliminate the remaining salts. A final wash in 100% acetone was used to prepare a very dense acetone precipitate of acid-oxidized, non-reticulated collagen, with no trace of undesirable chemical products (Tinois *et al.*, 1991). The precipitate was finally suspended in demineralized water at a concentration of 1% w/v and stored at 4°C.

2.4. Preparation of poly-(L-lactic acid) (PLLA) scaffold

A 3D PLLA–collagen scaffold was manufactured that had a unique structure, having collagen sponges formed within the pores of a mechanically strong knitted mesh of PLLA, as shown in Figure 1. Briefly, a 3D knit was prepared on a double-needlebar Raschel knitting machine, with six guide bars. Each of the faces of the knit, *i.e.* the first face and the second face, was prepared with two guide bars. The first face was prepared with bars B1 and B2, and the second, opposite, face was prepared with bars B5 and B6, each bar being threaded one full, one empty.

Bars B1 and B2, and B5 and B6, which produce the first and second faces of the knit, were threaded with PLLA 83.3 dtex multifilament yarn (decitex count 83.3 g/10,000 m yarn). The spacer was prepared using bars B3 and B4, threaded one full, one empty.

Bar B3 was threaded with PLLA 220 dtex monofilament yarn, so as to give thickness and resilience to the 3D knit. Bar B4 was threaded with PLLA 83.3 dtex multifilament yarn so as to give greater opacity between the faces.

The filament diameter of the multifilament yarns and the monofilament yarns were approximately 18 and 220 μm, respectively (Figure 1) and produced an isoelastic mesh of the following characteristics: weight/surface area of 116.5 g/m^2; macro pore size approximately 2×2 mm; thickness 3.1 mm; and 3D porosity 97%.

2.5. Preparation of PLLA mesh–collagen composite scaffolds

Porcine collagen that was GTA-crosslinked or oxidized (representing both long and short-term degradation profiles, respectively; modification proportions of 80:20 and 50:50 were studied) were mixed at a ratio of either 80:20 or 50:50, respectively, and poured over the 3D PLLA mesh to completely cover it (note: the topside of the scaffold is referred to as the 'sponge side', whilst the lower side will be referred to as the 'mesh side', in the remainder of the paper). The scaffold was lyophilized for 24 h and then sterilized by γ-irradiation at a minimum dose of 25 kGy. The precise scaffold architecture was defined by selecting the collagen mixture ratio, crosslinking density and yarn filament structure that achieved the best mechanical properties and *in vivo* biological performance (Pu *et al.*, 2010). The three scaffolds compared in this study were: PLLA coated with unmodified collagen that did not form a secondary 3D structure (scaffold A); PLLA with low-dose Oxicol and high-dose GTA (scaffold B); and PLLA coated with high-dose Oxicol and low-dose GTA (scaffold C). These are detailed in Table 1.

2.6. Scanning electron microscopy (SEM)

The structures of the PLLA–collagen scaffolds with and without cells were determined using a field emission scanning electron microscope (FE-SEM; LEO 1550, Cambridge, UK). Briefly, small pieces of the scaffold were coated with chromium (approximately 50 nm thick) under 125 mA. The coated samples were placed in the vacuum chamber of the FE-SEM and viewed at a voltage of 5 kV.

2.7. Isolation and culture of cells

2.7.1. Porcine bSMCs

Fresh porcine bladder specimens were collected in sterile phosphate-buffered saline (PBS). The bladder was cut in half and the urothelial layer peeled off from the luminal surface of the bladder under sterile conditions. The bladder muscle tissue was cut into small pieces, re-immersed in collagenase solution (2 mg/ml collagenase type IV) and then incubated at 37°C for 40 min on a roller-mixer. The supernatant was aspirated and complete medium added [Dulbecco's modified Eagle's medium (DMEM) containing 10% fetal calf serum (FCS) and penicillin–streptomycin]. The bladder pieces were minced evenly onto 150 mm tissue culture dishes in a few drops of complete medium and incubated at 37°C, 5% CO_2, for 30 min to promote tissue adherence. Complete medium was then added and the dishes returned to the incubator. The medium was replaced every 2–3 days until 80% confluence had been achieved,

at which point the cells were split at a ratio of 1:3. Cells at passages 4–6 were used for these studies. Morphological examination and immunohistochemical staining for αSMA were used to confirm the cell identity and homogeneity of the cultures.

2.7.2. C2C12 myoblasts

Undifferentiated myoblasts from a cell line originating from mouse skeletal muscle (ATCC) were grown in DMEM supplemented with 10% FCS and antibiotics [growth medium (GM)] at 37°C and 5% CO_2. The differentiation medium (DM) contained 2% horse serum instead of 10% FCS. The cells were passaged by trypsinization (0.5% trypsin in 0.5 mM EDTA; Gibco, UK) from the culture plate at 70% confluence. To demonstrate active C2C12 differentiation, cells were seeded at a density of $5 \times 10^4/cm^2$ and cultured to 70% confluence in DMEM and 10% FCS, followed by DM for 5 days.

2.8. Scaffolds and cell seeding

The 3D composite sponges, 2–3 mm thick, were fabricated as 15 mm diameter discs. The different formulations of crosslinking and oxidation of the porcine collagen are listed in Table 1. To evaluate cell adhesion, proliferation, phenotype and protein expression on the scaffold, bSMCs were seeded at a density of 105/scaffold in a 24-well plate and cell viability, proliferation, immunohistochemical staining and western blotting were evaluated at 1, 7 and 21 days.

To assess whether the scaffolds supported myogenic differentiation, myoblasts were seeded at a density of 5×10^5/scaffold and incubated in GM overnight, then in DM for 7 days. Cells were analysed for the expression of myogenic genes and protein expression by quantitative RT–PCR and immunohistochemical staining, respectively.

2.9. Cell viability and cell proliferation assay

A two-colour fluorescence cell viability assay was used, based on the ability of calcein AM to be retained within live cells, inducing an intense uniform green fluorescence and ethidium homodimer (EthD-1) to bind the nuclei of damaged cells, thus producing a bright red fluorescence in dead cells. Cell-loaded scaffolds were washed with PBS for 5 min and then submerged in a live/dead staining solution containing 2 μM calcein AM and 4 μM EthD-1. The samples were incubated for 30 min at 37°C, 5% CO_2 in the dark. Fluorescence images were acquired immediately using a laser scanning confocal microscope (Carl Zeiss 510).

To analyse the proliferation of porcine bSMCs following their seeding on the different scaffolds, a CyQUANT cell proliferation assay kit was used (Molecular Probes, Invitrogen, UK). The basis for the CyQUANT assay is the use of a proprietary green fluorescent dye (CyQUANT GR dye) that exhibits strong enhancement of fluorescence when bound to cellular nucleic acids. Cells were lysed with a buffer containing CyQUANT GR dye. Fluorescence was measured using an FLX800 fluorimeter (Bio-Tek Instruments), with excitation at 485 nm and emission at 530 nm. Sample fluorescence values were converted into cell numbers from a bSMC reference standard curve. The results are presented as a mean of four experiments ± standard error of the mean (SEM).

2.10. Quantitative RT-PCR

To determine myogenic gene expression by quantitative RT–PCR, total RNA was isolated at various time points, using an RNeasy Mini Kit (Qiagen) according to the manufacturer's protocol. Total RNA (1 μg) was reverse-transcribed to cDNA, using SuperScript^{TM} III reverse transcriptase and oligo(dT) (Invitrogen, UK) in a total reaction volume of 20 μl. The amplification was performed with a LightCycler 480 SYBR Green I Master (Roche Diagnostics). Amplification included a denaturation step at 95°C for 5 min, followed by 45 cycles at 95°C for 10 s, 55°C for 15 s and 72°C for 20 s. To verify amplification specificity, melting curves of the PCR products of each primer set were analysed. Each experiment was prepared in triplicate and data represented as mean ± standard deviation (SD) of four independent experiments. The sequences of the primers used are shown in Table 2. Relative expression level was computed for the RT–PCR data by the $\Delta\Delta C_T$ method, using GAPDH as the reference gene (Livak and Schmittgen, 2001; Pfaffl, 2002). All measurements of C_T values for each determination of the reference and experimental gene expression were performed in triplicate.

2.11. Immunohistochemical staining and western blotting

Cell-laden scaffolds or cell cultures on tissue culture plastic were fixed in 4% formaldehyde, blocked with normal horse serum and incubated with the appropriate antibody. For the study of bSMCs, SMC-specific contractile filament protein αSMA (1A4, 1:200; Sigma, UK) and smooth muscle myosin heavy chain (SM-MHC, G-4, 1:400; Santa Cruz Biotechnology) monoclonal antibodies were used. To determine myogenic differentiation, monoclonal antimyosin heavy chain II (MyHC, 1:400; Abcam, UK) was utilized. Immunohistochemical staining was achieved using a secondary biotinylated antibody (1:200), followed by a

Vectastain ABC-AP kit (AK5000, Vector Laboratories, UK) and the addition of the appropriate AP substrate (SP5000), to which levamisole solution had been added. Colour was developed for 20 min. Cell nuclei were stained by 4′-6-diamidino-2-phenylindole (DAPI; Vector Laboratories). Negative controls were for an anti-rabbit IgG, or deletion of the primary antibody in experiments where a secondary antibody was used. Images were acquired using laser scanning confocal microscopy (LSM 510, Zeiss, Germany).

Quantitative analysis of αSMA protein was performed using western blotting. bSMCs were cultured on PLLA–collagen scaffolds for up to 21 days and then washed twice with PBS and lysed in 400 μl Tris lysis buffer (0.01 M Tris, pH 7.4, and 1% sodium dodecyl sulphate). Following centrifugation, the protein concentration was determined by Bradford assay (Sigma, UK) with bovine serum albumin (BSA) as the standard. To detect protein expression, 30 μg total protein was separated by 10% SDS–PAGE. The protein fraction was transferred to a nitrocellulose membrane (Sigma), blocked with 3% BSA in 1× Tris-buffered saline with Tween (TBST; 10 mM Tris, 150 mM NaCl, 0.1% Tween-20) for 1 h at room temperature and then probed overnight with anti-αSMA monoclonal primary antibody (1:500; Abcam). HRP-conjugated secondary antibody (Santa Cruz Biotechnology) was incubated with the membranes for 1 h. Equal protein loading for these samples was confirmed by examining GAPDH expression. The chemiluminescent detection system ECL/ECL (Geneflow) enabled visualization following exposure to X-ray film. Autoradiographs were quantified by densitometry, using the Synoptics Group gene tools BioImaging system software (Syngene, Cambridge, UK) according to the manufacturer's instructions.

2.12. Statistical analysis

Statistical analysis was performed using SPSS v. 17 (Statistical Analysis Software, NC, USA). Data of gene expression and cell numbers were presented as arithmetic mean ± SD. For descriptive data, statistical evaluation was achieved by analysis of variance (ANOVA) with Tukey and Waller–Duncan's multiple comparison tests being applied to detect differences between groups. Four repeats/material/time period were assessed. In all statistical evaluations, $p<0.05$ was considered statistically significant.

3. Results

3.1. Characterisation of PLLA-collagen scaffolds

The morphology of the PLLA–collagen scaffolds, as observed by SEM, are displayed in Figure 1. PLLA mesh coated with collagen (scaffold A, Figure 1a–c) is a bundle-knitted structure having a wide texture (Figure 1a) with a fibre diameter of approximately 20 μm (Figure 1b) and comprising various sheet structures (Figure 1c). PLLA–collagen composite (lower-dose Oxicol, scaffold B; Figure 1d–f) has collagen filaments masking the bundle-knitted structures (Figure 1d). In this formulation, collagen is more abundant on the top surface than on the bottom (Figure 1f). In addition, the scaffold surface was largely covered by the collagen coating (Figure 1e). A similar situation was observed in scaffold C (Figure 1g–i, higher-dose Oxicol). Collagen sponges with interconnected micropores formed in the interstices of the synthetic polymer mesh. The polymer mesh was embedded in the collagen sponge, such that the polymer fibre bundles and the collagen sponges were alternately chained. Observation by SEM demonstrated that the pores were distributed evenly in the scaffolds that had collagen sponges (scaffolds B and C). This was confirmed by micro-computed tomography (μCT) analysis. The degree of porosity was determined to be approximately 81% and the mean pore size 110 μm. In addition, the 3D scaffold was constructed with bioresorbable material which has an expected *in vivo* degradation time in the range ca. 3 months–2 years, as previously reported for crosslinked collagens (Paul and Bailey, 2003) and for Oxicol scaffolds (Pu *et al.*, 2010). The mesh has isoelastic mechanical properties in the range suitable for tissue-engineering applications.

3.2. Characterisation of primary-derived bSMCs

bSMCs were successfully established from porcine bladders. Following isolation, the bSMCs adhered and grew out from the bladder tissue during the first 2 days and multiplied rapidly to form uniform spindle-shaped cells, which were identified by phase-contrast microscopy (Figure 2a). Isolated primary cells can be identified by their affinity to antibodies against αSMA; > 95% of the cultured bSMCs stained positively for αSMA. bSMCs expressed prominent αSMA-labelled thick filaments in the cytoplasm (Figure 2b). Confluent monolayers of bSMCs exhibited characteristic ‘hill and valley’ morphology in culture and expressed SM-MHC (Figure 2c).

3.3. Viability, proliferation and distribution of bSMCs on scaffolds

bSMCs were viable after seeding on 3D scaffolds during the experimental period. After 1 day in culture (Figure 3a–c), cells adhered to the scaffolds, but many were not well spread. Over time, the cell numbers increased and were evenly distributed throughout the scaffolds. Up to

14 days (Figure 3d–f), cells grew rapidly on the scaffolds that had collagen sponge (scaffolds B and C) compared to scaffold A, which did not, and which had a greater number of dead cells. Moreover, the cells were distributed to the bottom of scaffold C compared to scaffold B.

As observed using SEM, scaffold C was covered by a dense cell layer on its surface after 7 days. In contrast, the surface of scaffolds A and B exhibited less cell coverage of the top surface and only a few cells observed on the under-surface. By 21 days, the bSMCs had formed a confluent layer covering both surfaces on scaffold C (Figure 3i, l), suggesting that cells were able to migrate throughout the scaffold and fill the entire construct. In contrast, only 60% of the surface of scaffold B was covered by cells (Figure 3h, k). Scaffold A only had a few cells on its fibres (Figure 3g, j), suggesting that the structure had severe limitations in supporting cell growth.

At day 1, the number of cells, as measured by the CyQuant assay, that were adhered to both scaffolds B and C (sponge-filled) were significantly greater than on scaffold A (Figure 3n). This was observed also on days 7 and 21. After 7 days, scaffold C had the highest cell numbers, although the numbers of cells had also increased slightly on scaffold A. At day 21, cell proliferation rates were significantly higher ($p<0.001$) in scaffold C, whereas cell numbers had plateaued by 7 days in scaffold B.

3.4. Expression of α-SMA on bSMCs

Expression of αSMA, a marker of SMCs, is shown in low (Figure 4a, c, e) and high (Figure 4b, d, f) magnifications. The cells cultured on scaffold C showed intense staining for αSMA (Figure 4f, g), demonstrating that this scaffold not only supports cell proliferation but also sustains the smooth muscle cell phenotype, which has muscle function. To further confirm these results, αSMA protein production in the scaffolds was investigated by western blotting at 21 day (Figure 4g). A two-fold increase in αSMA protein expression was demonstrated on scaffold C compared to scaffold A. This result further confirms that PLLA–collagen scaffold with the higher dose of Oxicol is best at supporting cell growth whilst maintaining the specific SMC phenotype.

3.5. Characterisation of myoblast differentiation

Undifferentiated C2C12 myoblasts (Figure 5a) cultured in differentiation medium for 5 days demonstrated the presence of multinucleated, elongated myotubes under phase-contrast light microscopy (Figure 5b). During this culture period, expression of the MRF genes myogenin

and MFR4 was significantly increased, by a factor of 26 and 141, respectively, compared to undifferentiated cells (Figure 5c). Expression of the proliferation marker MyoD did not change.

3.6. Myogenic differentiation and myotube formation

C2C12 myoblasts seeded on the scaffolds in differentiation media and cultured for 7 days were analysed by quantitative RT–PCR (Figure 6a). The expression of MyoD was at its highest intensity at day 1 compared to day 7 for all scaffolds. After 1 day in myogenic differentiation culture, MyoD expression was 2.65- and 2.80-fold greater in scaffolds B and C, respectively, than in scaffold A, which was 1.59-fold higher than the baseline of the uncommitted cells (Figure 6a). Expression of the late myogenic markers myogenin and MFR4 increased significantly at day 7 compared to day 1. Following 7 days of myogenic induction, upregulation of myogenin had increased 26-fold on scaffold C, whilst MFR4 was expressed 167-fold higher. These figures are 1.5 and 3.85 times greater than those observed for scaffold A. Statistically, expression of myogenin and MFR4 mRNA was significantly different within the group ($p<0.001$; Figure 6a), indicating that scaffold C supportedmyogenic differentiation into the later stages better than the other scaffolds.

To further confirm the results of the quantitative RT–PCR analysis, the capability of the C2C12 cells to fuse and differentiate into multinucleated myotubes on the 3D scaffolds was further investigated by means of immunofluorescent staining for MyHC. MyHC is expressed in terminally differentiated skeletal muscle cells and is a late marker of myogenic commitment. The expression of MyHC was observed mostly in multinucleated myotubes. Cells were seen to adhere and proliferate throughout the scaffold. Figure 6b shows evidence of cell nuclei lining up along the direction of the scaffold fibres, suggesting the presence of multinucleated myotubes running parallel to the scaffold fibrous structure. This supposition was confirmed by observation of myosin expression (MyHC; Figure 6b, stained red, cell nuclei in blue) when cultured in DM for 7 days. A high degree of orientation of myotubes was observed in cells on scaffold C (Figure 6b). Conversely, few myotubes were expressed in scaffolds A or B.

4. Discussion

The design and selection of a biomaterial for engineering muscular tissues requires appropriate regulation of cell behaviour (e.g. adhesion, proliferation, migration and differentiation) to promote the development of functional new tissue in the absence of adverse host reactions (*e.g.* inflammation). This study demonstrated that biodegradable collagen–PLLA composite

scaffolds combined with a novel collagen formulation fully supports the maturation and differentiation of SMCs and myoblasts, strongly suggesting that these scaffolds, by virtue of their specific formulation and design, are good candidates for the reconstruction of muscular tissue defects, in particular the abdominal wall and bladder, through enhancement of the regeneration of both skeletal and smooth muscle components. PLLA–collagen scaffold comprising higher-dose Oxicol sponge provided the best results, not just in its ability to sustain myogenic differentiation and myotube formation, but also in supporting bSMC cell adhesion and proliferation and also the secretion of SMC functional proteins, which were strongly expressed, as determined by immunofluorescence and western blotting.

The repair of large, complex abdominal wall defects is often compromised by factors related to the health of the patient, including diabetes, which is implicated in exacerbated wound bacterial contamination and obesity, resulting in impaired wound healing. Diabetic patients suffer impaired endothelial progenitor cell (EPC) recruitment from the bone marrow, due to reduced SDF-1α expression in the myofibroblastic cell population (Brem and Tomic-Canic, 2007). The reduced numbers of EPCs result in reduced vasculogenesis and therefore reduced peripheral blood flow, resulting in a diminished local wound-healing response. This reduced blood flow further decreases the ability of diabetic patients to fight bacterial contamination, meaning that wounds are more likely to become contaminated, further hindering normal wound healing. The presence of wound contamination is particularly problematic, as subsequent necrosis dramatically increases wound closure-failure rates. Of course, any condition that increases intra-abdominal pressure, including obesity and chronic pulmonary disease, is additionally liable to result in increased defect repair-failure rate. Furthermore, patients using corticosteroids also have impaired abdominal wall physiology (Ehrich and Hunt, 1968; Wicke *et al.*, 2000).

The abdominal wall comprises six layers: skin, subcutaneous fascia, musculature, transversalis fascia, preperitoneal tissue and peritoneum. The musculature consists of a group of skeletal muscles which work in concert to provide the mechanical strength and flexibility necessary to move the torso, in addition to performing the primary function of the abdominal wall, counteracting the large pressure force exerted by the internal organs. Loss of this musculature is critical, as the muscles provide the majority of the abdominal wall's mechanical strength. Skeletal muscle provides the bulk of the mechanical strength, mobility and flexibility of not only the abdominal wall but also the majority of the mobile components of the body.

Skeletal muscle fibre development and regeneration are similar processes. In development, mononuclear myoblasts line up parallel to one another and fuse to produce

multinucleated myotubes. The myotubes share the cytoplasm of the incorporated myoblasts and their nuclei are dispersed along its length. Once the myotubes are formed, they undergo a maturation process, during which they become innervated and vascularized, resulting in myofibres (Wilson *et al.*, 1992). The parallel alignment of the myoblasts during fusion is key to the myofibres' ability to produce the necessary force for movement and strength. Muscle regeneration and repair following trauma to the abdominal wall commences with the activation of satellite progenitor cells (Chen and Goldhamer, 2003; Dhawan and Rando, 2005; Wagers and Conboy, 2005). Once activated, these satellite cells migrate to the site of the defect and proliferate. Within the defect they create new myotubes by aligning parallel to the injured myofibres, and fuse to each other. These myotubes mature through innervation and vascularization to become functioning myofibres. Skeletal muscle tissue engineering depends on the regenerative properties of the satellite cells and their potential to proliferate and differentiate to form organized structures. Previous skeletal muscle tissue-engineering studies have focused on either the ability of muscle cells to contract engineered substrates or their potential to form myotubes whilst being cultured on those biomaterials (as films, hydrogels or nanofibres; Borschel *et al.*, 2006; Kamelger *et al.*, 2004; Saxena *et al.*, 1999, 2001).

In this study we report that the 3D PLLA–collagen scaffolds support enhanced myogenesis, especially those with an increasing ratio of oxidized collagen, with the differentiation of C2C12 cells to skeletal myoblasts and the formation of myotubes. In terms of cell differentiation, quantitative RT–PCR analysis of C2C12 myoblasts cultured on the scaffolds demonstrated expression of typical myogenic markers (MyoD, myogenin and MRF4). The scaffolds with higher-dose Oxicol sponge induced the greatest myogenesis, having the highest expression of the late myogenic markers myogenin and MRF4. Furthermore, the presence of MyHC in C2C12 cells cultured on this scaffold was clearly confirmed by subsequent immunofluorescent staining, demonstrating the development of multinucleated myosin-expressing myotubes. The design of the 3D composite sponges described in this study has allowed the possibility of the degradation rate to be tailored to the precise clinical application, having a combination of collagen modifications with differential degradation kinetics. Furthermore, we have demonstrated that sponges with higher-dose Oxicol facilitated myogenic differentiation and myotube formation.

The myogenic response of the higher dose of oxidized collagen in the Oxicol scaffolds may be due to the change in surface topography that the specific ratio of GTA:oxidized collagen has caused. SEM observation of the high-dose oxidized collagen formulation clearly shows the presence of small-diameter fibres on the surface. Dang and Leong (2007) found that

the topographical features of nanofibres having a diameter of several hundred nanometers was responsible for the myogenic induction of human mesenchymal stem cells (hMSCs) in *in vitro* culture. The precise mechanism of myogenic induction in C2C12 cells following culture on Oxicol scaffolds requires further investigation, as so far there has been no literature published which reports the effect of oxidation of collagen on induced myogenesis.

Additionally, the 3D scaffolds were constructed so as to satisfy the criteria for bladder tissue engineering. Such scaffolds must be able to support the adhesion and proliferation of a number of cell types, including urothelial cells on the luminal side and smooth muscle cells surrounding the urothelial barrier. They must also be able to direct tissue maturation suitable for the formation of a functional bladder. It has been reported that many naturally derived and synthetic biomaterials, including collagen and PLLA, exhibit adequate *in vitro* biocompatibility for a large range of cell types, including bladder cells (Kim *et al.*, 2000; Pariente *et al.*, 2002). In this study, the 3D PLLA–collagen scaffolds facilitated effective seeding of primary smooth muscle cells derived from the porcine bladder. However, the cell population developed more satisfactorily in scaffolds that incorporated a collagen sponge than those without, improving the cell seeding and proliferation of bladder SMCs. The collagen sponge prepared with higher-dose Oxicol demonstrated better cell growth profiles than the lower-dose variants, suggesting that the higher dose favours cell adherence and proliferation. Previous research has demonstrated that vascular smooth muscle cells proliferate more actively when seeded on the surface of oxidized than unmodified collagen (Bacáková *et al.*, 1997), although the mechanism of stimulation remains to be elucidated. It has been suggested that in SMC, oxidized low-density lipids stimulate mitogen-activated protein kinases (Chatterjee *et al.*, 1997), and reactive oxygen species, such as superoxide anion, hydrogen peroxide and hydroxyl radicals increase autocrine production of mitogens, *e.g.* insulin-like growth factor (Bacáková *et al.*, 1999). Similar effects could also be induced by Oxicol. Furthermore, the highest expression of the SMC functional marker αSMA was observed on this combined scaffold. As a result, the combination of PLLA mesh and collagen sponge with higher-dose Oxicol developed in this research is likely to be a valuable biomaterial for the regeneration of bladder tissue.

For clinical applications, these scaffolds may be deployed in acellular form, without the additional seeding of cells or pre-seeded with autologous cells. The ability of the scaffolds to support enhanced cellular adhesion, proliferation and differentiation compared to conventional mesh biomaterials suggest that use of the device in a clinical setting will enhance tissue

regeneration of skeletal and smooth muscle applications, such as abdominal wall defect and bladder repair.

C2C12 is a permanent cell line derived from mouse skeletal muscle (Yaffe and Saxel, 1977). These cells were used for this study because of their reliability, easy availability and ease of culture. Although C2C12 cells differentiate rapidly, form contractile myotubes and produce proteins characteristic of the muscle (Bains *et al.*, 1984; Bennett and Tonks, 1997), C2C12 myooids possess less contractility than those from primary skeletal muscle cultures (Dennis and Kosnik, 2000; Dennis *et al.*, 2001). However, previous studies using these cells suggest that the profile of maturation will be replicated in primary cultures. Future studies will focus on scaffold contractility and structure, using primary cells from primary mammalian skeletal muscle, and investigate the effect of mechanical conditioning on cell–scaffold constructs and to quantify their mechanical properties and active force capabilities. Additional clinical applications, such as congenital diaphragmatic hernia, may also be investigated.

5. Conclusion

In this study, we have demonstrated that the incorporation of higher-dose Oxicol within biodegradable PLLA–collagen scaffolds improves cell adhesion, proliferation and uniform distribution throughout the entire 3D collagen sponge for all of the cell types studied. The 3D scaffolds demonstrated enhanced myogenic differentiation and myotube formation through the expression of myogenic regulator genes and proteins, compared to simple 3D scaffolds constructed from PLLA and coated with unmodified collagen. The results suggest that these Oxicol scaffolds would enhance clinical reconstruction of abdominal wall defects. In addition, the greater αSMA protein expression, enhanced cell proliferation and sustained SMC phenotype promoted by this scaffold suggests that bSMCs grown on the scaffolds clinically are likely to have smooth muscle function. Together, our results indicate that these 3D biodegradable scaffolds constructed from PLLA textiles and high-dose Oxicol sponges can be used for the engineering of both smooth and skeletal muscle tissue, extending their role in regenerative medicine.

Acknowledgements

This study was supported by European Commission, project number PPCOO-2106. Parts of the research were performed as part of the Interdisciplinary Research Collaboration in Tissue Engineering for which funds were provided by the BBSRC, MRC and EPSRC.

References

Afanasiev P, Thiollier A, Breysse M, *et al*. 1999; Control of the textural properties of zirconium oxide. *Top Catalysis* **8**: 147-160.

Arrow, AK. 2001; *Biotechnology in wound care, investment outlook*. Los Angeles: Wedbush Morgan Stanley Securities. pp 1–82.

Bacáková L, Herget J, Wilhelm J. 1999; Influence of macrophages and macrophage- modified collagen I on the adhesion and proliferation of vascular smooth muscle cells in culture. *Physiol Res* **48**: 341-351.

Bacáková L, Wilhelm J, Herget J, *et al*. 1997; Oxidized collagen stimulates proliferation of vascular smooth muscle cells. *Exp Mol Pathol* **64**: 185-194.

Bains W, Ponte P, Blau H, *et al*. 1984; Cardiac actin is the major actin gene product in skeletal muscle cell differentiation in vitro. *Mol Cell Biol* **4**: 1449-1453.

Bellon JC. 2007; *Biological reasons for an incisional hernia*; in: Recurrent Hernia. Eds. V Schumpelick, RJ Fitzgibbons. Springer Medizin. pp129-133.

Bennett AM, Tonks NK. 1997; Regulation of distinct stages of skeletal muscle differentiation by mitogen-activated protein kinases. *Science* **278**: 1288-1291.

Blatnik J, Jin J, Rosen M. 2008; Abdominal hernia repair with bridging acellular dermal matrix – an expensive hernia sac. *Am J Surg* **196**: 47-50.

Borschel GH, Dow DE, Dennis RG, *et al*. 2006; Tissue engineered axially vascularized contractile skeletal muscle. *Plast Reconstr Surg* 7: 2235-2242.

Brem H, Tomic-Canic M. 2007; Cellular and molecular basis of wound healing in diabetes. *J Clin Invest* **117**: 1219-1222.

Burger JW, Luijendijk RW, Hop WC, *et al*. 2004; Long-term follow-up of a randomized controlled trial of suture versus mesh repair of incisional hernia. *Ann Surg* **240**: 578-583.

Carlson MA. 1997; Acute wound failure. *Surg Clin North Am* **77**: 607-636.

Cassar K, Munro A. 2002; Surgical treatment of incisional hernia. *Br J Surg* **89**: 534-545.

Chatterjee S, Bhunia AK, Snowden A, *et al*. 1997; Oxidized low density lipoproteins stimulate galactosyltransferase activity, ras activation, p44 mitogen activated protein kinase and c-fos expression in aortic smooth muscle cells. *Glycobiology* **7**: 703-710.

Chen JC, Goldhamer DJ. 2003; Skeletal muscle stem cells. *Reprod Biol Endocrinol* **1**: 101.

Dang JM, Leong KW. 2007; Myogenic induction of aligned mesenchymal stem cell sheets by culture on thermally responsive electrospun nanofibers. *Adv Mater* **19**: 2775-2779.

Dhawan J, Rando TA. 2005; Stem cells in postnatal myogenesis: molecular mechanisms of satellite cell quiescence, activation and replenishment. *Trends Cell Biol* **15**: 666-673.

Dennis RG, Kosnik PE. 2000; Excitability and isometric contractile properties of mammalian skeletal muscle constructs engineered in vitro. *In Vitro Cell Dev Biol Anim* **36**: 327–335.

Dennis RG, Kosnik PE, Gilbert ME, *et al*. 2001; Excitability and contractility of skeletal muscle engineered from primary cultures and cell lines. *Am J Physiol Cell Physiol*. **280**: C288-295.

Ehrich HP, Hunt TK. 1968; Effects of cortisone and vitamin A on wound healing. *Ann Surg* **177**: 222-227.

European markets for soft tissue repair devices. 2009; *Millennium Research Group research report*.

Hodgson NC, Malthaner RA, Ostbye T. 2000; The search for an ideal method of abdominal fascial closure: a meta-analysis. *Ann Surg* **231**: 436-442.

Hoer J, Lawong G, Klinge U, *et al*. 2002; Factors influencing the development of incisional hernia. A retrospective study of 2,983 laparotomy patients over a period of 10 years. *Chirurg* **73**: 474-480.

Kamelger FS, Marksteiner R, Margreiter E, *et al*. 2004; A comparative study of three different biomaterials in the engineering of skeletal muscle using a rat animal model. *Biomaterials* **9**: 1649-1655.

Kim BS, Baez CE, Atala A. 2000; Biomaterials for tissue engineering . *World J Urol* **18**: 2-9.

Kingsnorth A. 2006; The management of incisional hernia. *Ann R Coll Surg Engl* **88**: 252-260.

Leber GE, Garb JL, Alexander AI, *et al*. 1998; Long-term complications associated with prosthetic repair of incisional hernias. *Arch Surg* **133**: 378-382.

Livak KJ, Schmittgen TD. 2001; Analysis of relative gene expression data using real-time quantitative PCR and the 2(T)(-Delta Delta C) method. *Methods* **25**: 402–408.

Luijendijk RW, Hop WC, van den Tol MP, *et al*. 2000; A comparison of suture repair with mesh repair for incisional hernia. *N Engl J Med* **343**: 392–398.

Mudge M, Hughes LE. 1985; Incisional hernia: a 10-year prospective study of incidence and attitudes. *Br J Surg* **72**: 70-71.

Park AE, Roth JS, Kavic SM. 2006; Abdominal wall hernia. *Curr Probl Surg* **43**: 326-375.

Parker MH, Seale P, Rudnicki MA. 2003; Looking back to the embryo: defining transcriptional networks in adult myogenesis. *Nat Rev Genet* **4**: 497–507.

Pariente JL, Kim BS, Atala A. 2002; In vitro biocompatibility evaluation of naturally derived and synthetic biomaterials using normal human bladder smooth muscle cells. *J Urol* **167**: 1867-1871.

Paul RG, Bailey AJ. 2003; Chemical stabilisation of collagen as a biomimetic. *Sci World J* **3**: 138–155.

Pfaffl MW. 2002; A new mathematical model for relative quantification in real-time RT-PCR. *Nucl Acids Res* **29**: 2002–2007.

Pownall ME, Gustafsson MK, Emerson CP. 2002; Myogenic regulatory factors and the specification of muscle progenitors in vertebrate embryos. *Annu Rev Cell Dev Biol* **18**: 747–783.

Pu FR, Rhodes NP, Bayon Y, Chen R, *et al*. 2010; The use of flow perfusion culture and subcutaneous implantation with fibroblast-seeded PLLA-collagen 3D scaffolds for abdominal wall repair. *Biomaterials* **31**: 4330–4340.

Santora T, Roslyn JJ. 1993; Incisional hernia. *Surg Clin North Am* **73**: 557–570.

Saxena AK, Marler J, Benvenuto M, *et al*. 1999; Skeletal muscle tissue engineering using isolated myoblasts on synthetic biodegradable polymers: preliminary studies. *Tissue Eng* **6**: 525-532.

Saxena AK, Willital GH, Vacanti JP. 2001; Vascularized three dimensional skeletal muscle tissue-engineering. *Biomed Mater Eng* **4**: 275-281.

Sorensen LT, Hemmingsen UB, Kirkeby LT, *et al*. 2005; Smoking is a risk factor for incisional hernia. *Arch Surg* **140**: 119-123.

Sugerman HJ, Kellum JM Jr, Reines HD, *et al*. 1996; Greater risk of incisional hernia with morbidly obese than steroid-dependent patients and low recurrence with prefascial polypropylene mesh. *Am J Surg* **171**: 80–84.

Tinois E, Tiollier J, Gaucherand M, *et al*. 1991; In vitro and post-transplantation differentiation of human keratinocytes grown on the human type IV collagen film of a bilayered dermal substitute. *Exp Cell Res* **193**: 310-319.

US markets for soft tissue repair devices. 2010; *Millennium Research Group research report*. 2010.

Valentin JE, Badylak JS, McCabe GP, *et al*. 2006; Extracellular matrix bioscaffolds for orthopaedic applications: a comparative histologic study. *J Bone Joint Surg A* **88**: 2673-2686.

Wagers AJ, Conboy IM. 2005; Cellular and molecular signatures of muscle regeneration: current concepts and controversies in adult myogenesis. *Cell* **122**: 659-667.

Wicke C, Halliday B, Allen D, *et al*. 2000; Effects of steroids and retinoids on wound healing. *Arch Surg* **135**: 1265-1270.

Wigmore OM, Dunglison GF. 1998; The generation of fiber diversity during myogenesis. *Int J Dev Biol* **42**: 117-125.

Wilson SJ, McEwan JC, Sheard PW, *et al*. 1992; Early stages of myogenesis in a large mammal: formation of successive generations of myotubes in sheep tibialis cranialis muscle. *J Musc Res Cell Motility* **13**: 534-550.

Yaffe D, Saxel O. 1977; Serial passaging and differentiation of myogenic cells isolated from dystrophic mouse muscle. *Nature* **270**: 725-727.

Table 1. Scaffolds used in the studies

Scaffolds	Structure	Sponge	Porosity (mesh)
Scaffold A (no sponge)	3D PLLA textile coated with Oxicol	Coated control	Multifilament fibers
Scaffold B (lower dose Oxicol)	3D PLLA textile coated with Oxicol	80% of GTA/ 20%of Oxicol	Monofilament fibers
Scaffold C (higher dose Oxicol)	3D PLLA textile coated with Oxicol	50% of GTA/ 50%of Oxicol	Multifilament fibers

Table 2. Primers used for real time RT-PCR analysis

Gene	Forward primer	Reverse primer	PCR cycles		Product (bp)
MyoD	CCAATGCGATTTATCAGGTG	GAAGAACCAGGGACACCATC	35	NM_010866	94
Myogenin	CCACAATCTGCACTCCCTTA	CTGGGAAGGCAACAGACATA	35	NM_031189	71
MHC (Myh2)	AACAGCAGCGACTGATCAAC	CGACTGCAGACCGAATCCGG	40	NM_001039545	137
Gapdh	CGTGTTCCTACCCCCAATGT	TGTCATCATACTTGGCAGGTTTCT	35	NM_001001303	128

Figure Captions

1. SEM micrographs of PLLA-collagen scaffold. Scaffold A (a-c). (a) Knitted mesh with coated collagen, Mag = 50x; (b) Mag = 500x; (c) Cross-section of mesh, Mag = 150x; Scaffold B (d-f). (d) Mesh with the collagen sponge (80:20, GTA crosslinked : oxidised collagen, Mag = 50x; (e) Mag = 500x; (f) Cross-section of the scaffold, Mag = 150x. Scaffold C, (g-i). (g) Mesh with the collagen sponge (50:50, GTA crosslinked : oxidised collagen, Mag = 50x; (e) Mag = 500x; (f) Cross-section of the scaffold, Mag = 150x

2. Characterization of porcine bladder smooth muscle (SM) cells (bSMCs). To confirm their SM cell phenotype, the cells were examined morphologically and by their protein expression. (a) bSMCs in culture - typical SM cell morphology; (b) inmmunostaining of α-SM actin on cultured bMSCs. α-SM actin expressed in red and cell nuclei in blue; (c) confluent monolayer of bSMCs exhibited a characteristic 'hill and valley' morphology in the culture and expressed SM-MHC (in red)

3. Viability and Proliferation of bSMCs on the scaffolds for up to 21 days. Confocal images of bSMCs cultured on scaffolds for 1 day (a-c) and 14 days (d-i); Cells stained green are live and red are dead.; SEM images of bSMCs grown on scaffolds for 21 days (g-l); Top side (g-i) and bottom side (j-l). (m) CyQUANT cell proliferation measurements of cell lysates from cell cultured on scaffolds. Cell-loaded scaffolds cultured after 1, 7 and 21 days, results represent mean and standard deviation, $n = 4$. p values show statistically significant differences among group (G) and day 1 (D). Error bars denote standard deviation, Scale bars represent 100 μm

4. Confocal images of α-SM actin protein expressed on bSMCs cultured on scaffolds for up to 21 days, low (a-c) and high magnification (d-f). (a, d) Scaffold A; (b, e) Scaffold B; (c, f) Scaffold C; (g, h) Western blot analysis of α -SMA on scaffolds seeded with bSMCs. Cellular protein extracted from cell-loaded scaffolds were size separated by SDS-PAGE and transferred to a nitrocellulose membrane for detecting α-SM actin (g). Arbitrary optical densitometry (OD) units from western blot of α-SM actin expression. $*p < 0.001$

5. Characterisation of C2C12 myoblast differentiation. Morphology of C2C12 myoblasts before and after differentiation, viewed using phase contrast microscopy. (a) Undifferentiated cells; (b) Differentiated C2C12 myoblasts demonstrating multinucleated, elongated myotubes; (c) Expression of myogenic differentiation factors on C2C12 myoblasts cultured in DM for 5 days and analysed by quantitative RT-PCR ($n = 3$)

6. (a) Expression of Myogenic differentiation factors MyoD, Myogenin and MRF4 on C2C12 myoblasts cultured in DM on scaffolds for 1 and 7 days analysed by quantitative RT-PCR for (*n = 3*); (b) Expression of MyHC detected by immunofluorescence staining (red) on C2C12 myoblasts cultured on scaffolds in DM for 7 days

Figure 1.

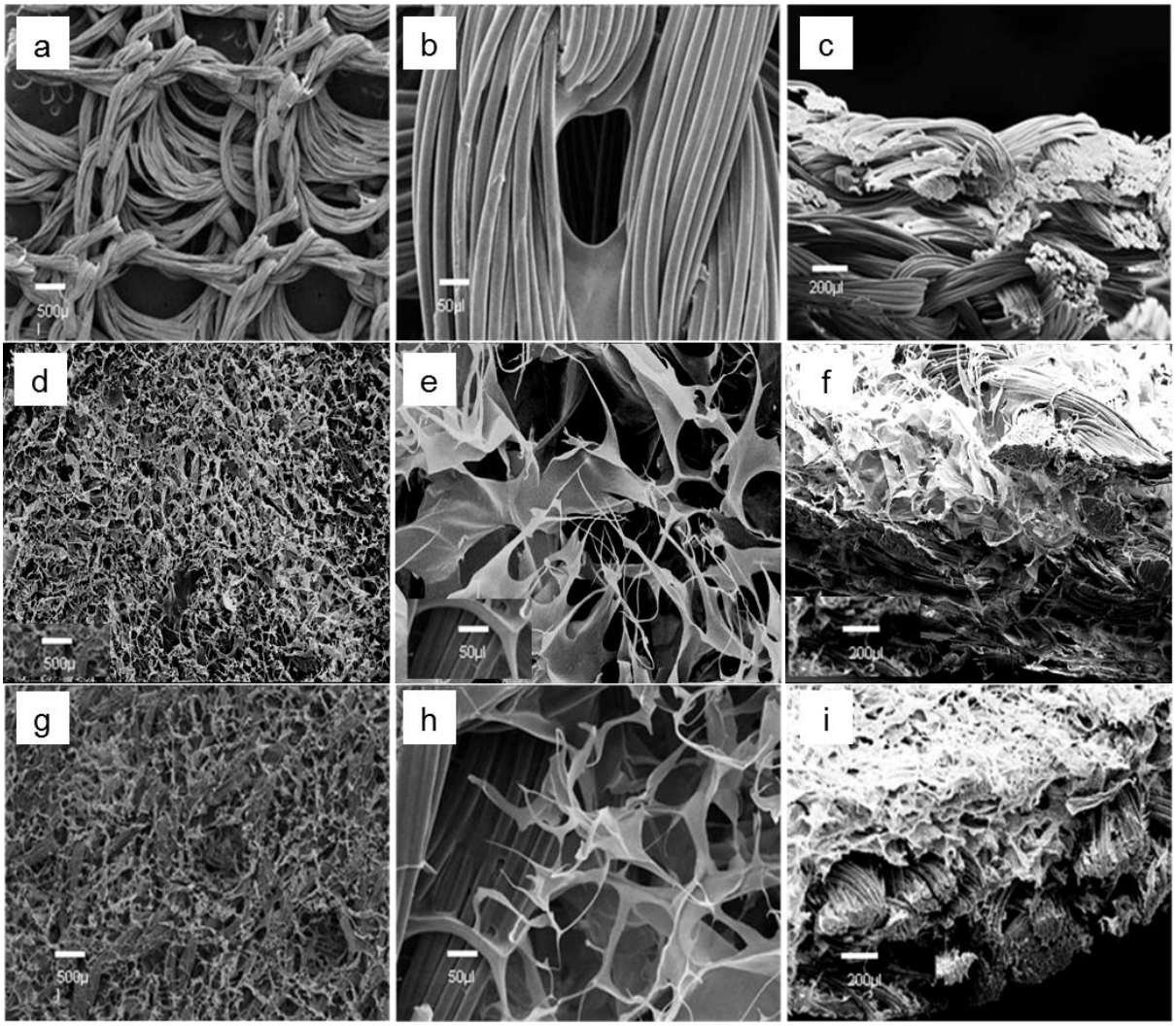

Figure 2.

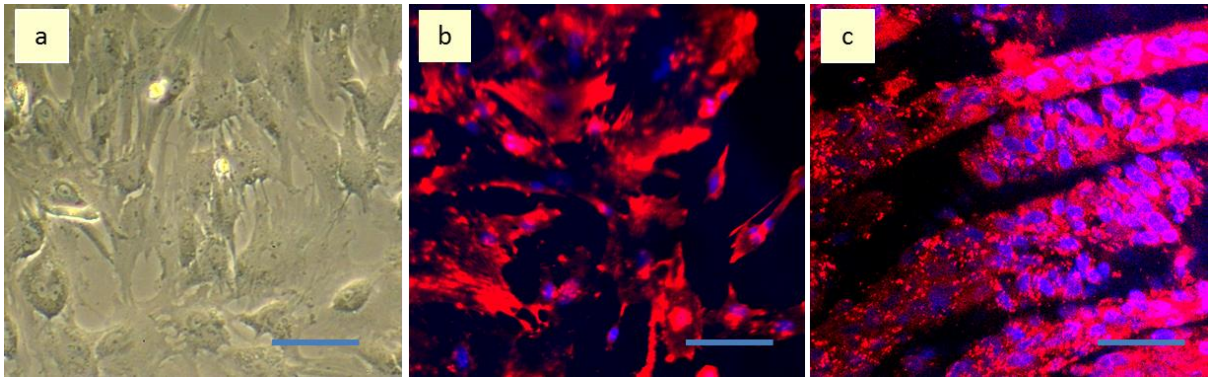

Figure 3.

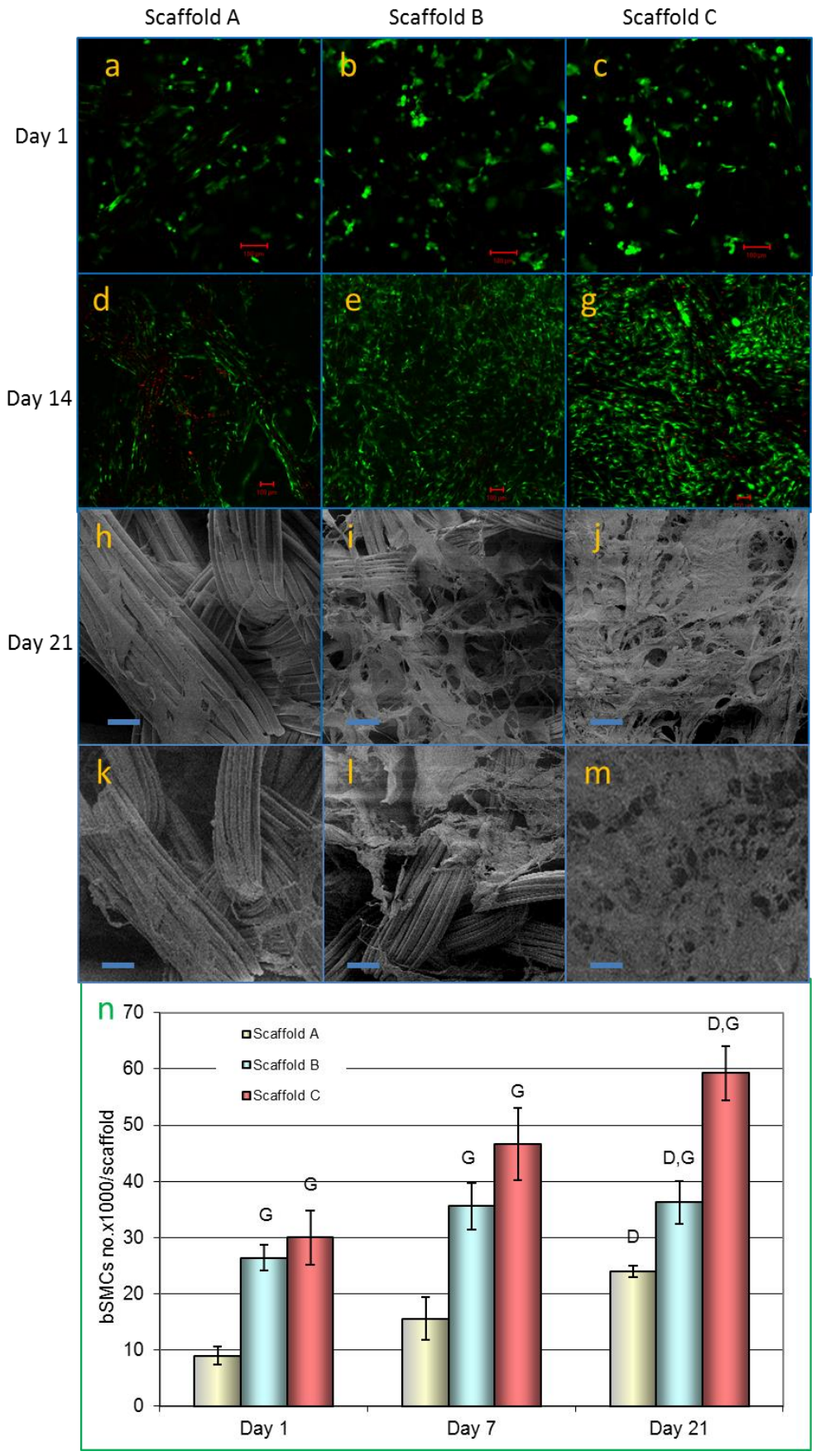
Scaffold A
Scaffold B
Scaffold C
Day 1
Day 14
Day 21
a
b
c
d
e
g
h
i
j
k
l
m
n
Scaffold A
Scaffold B
Scaffold C
bSMCs no.x1000/scaffold
0
10
20
30
40
50
60
70
G
G
G
G
D
D,G
D,G
Day 1
Day 7
Day 21

Figure 4.

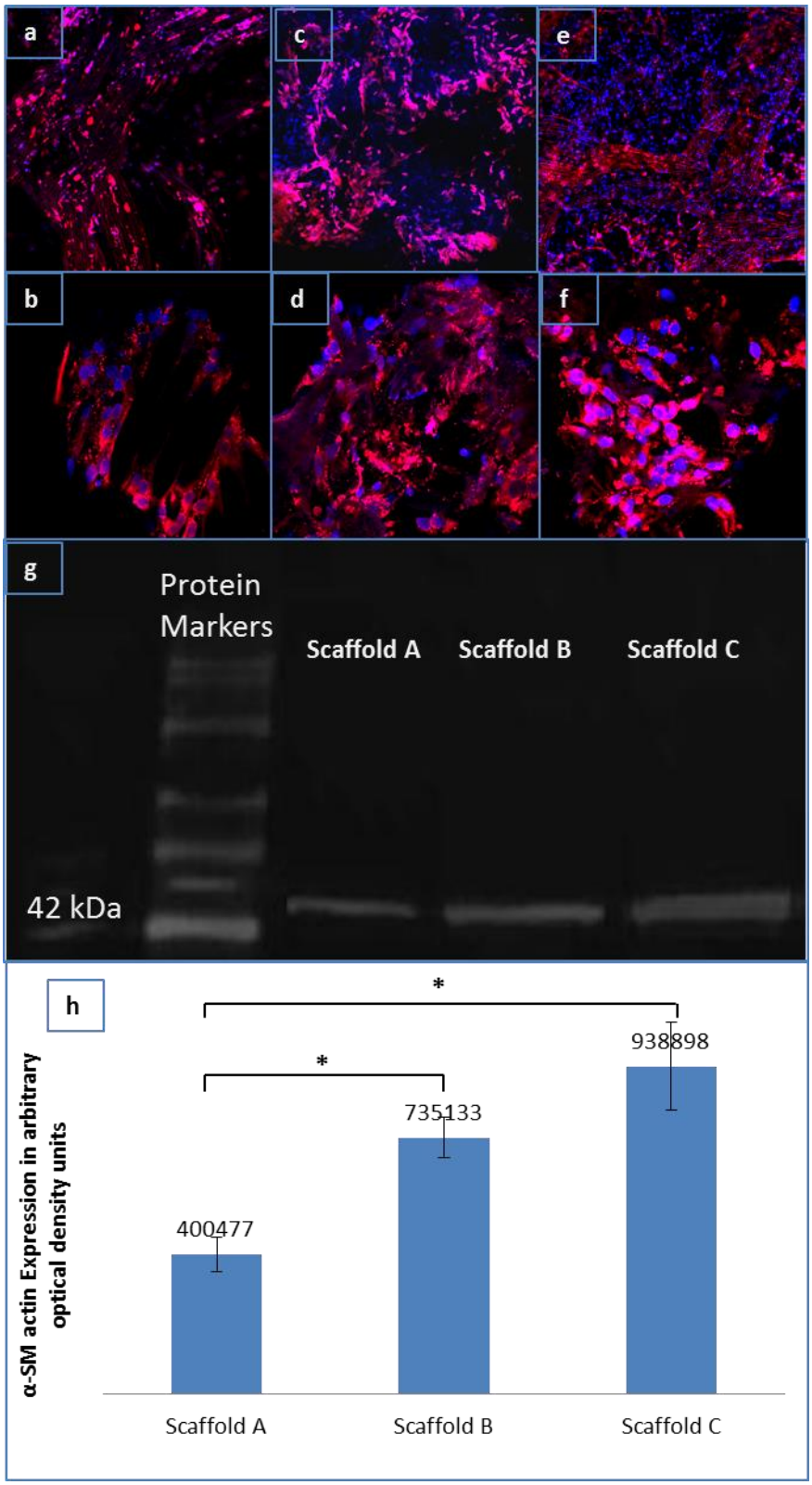
a
c
e
b
d
f
g
Protein Markers
Scaffold A
Scaffold B
Scaffold C
42 kDa
h
*
*
938898
735133
400477
α-SM actin Expression in arbitrary optical density units
Scaffold A
Scaffold B
Scaffold C

Figure 5.

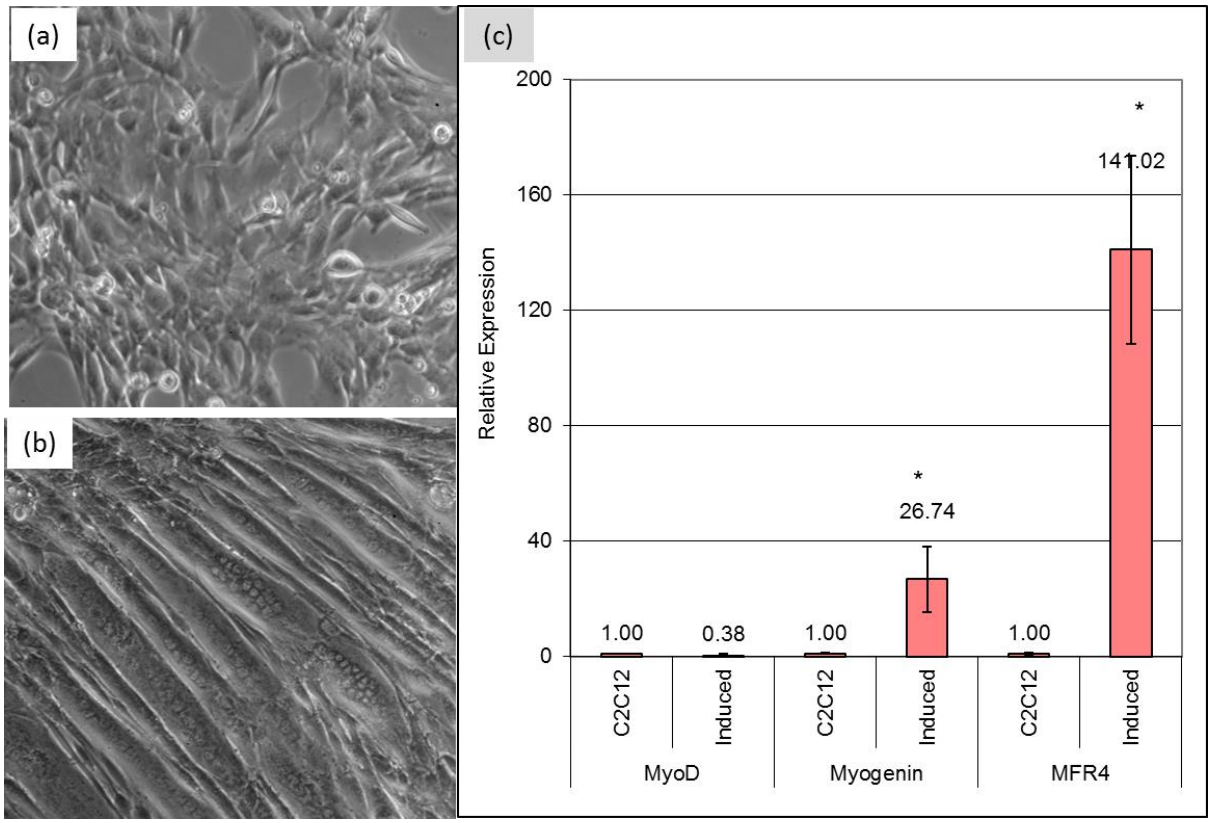
(a)
(b)
(c)
Relative Expression
200
160
120
80
40
0
1.00
0.38
1.00
26.74
1.00
141.02
*
*
C2C12
Induced
C2C12
Induced
C2C12
Induced
MyoD
Myogenin
MFR4

Figure 6.

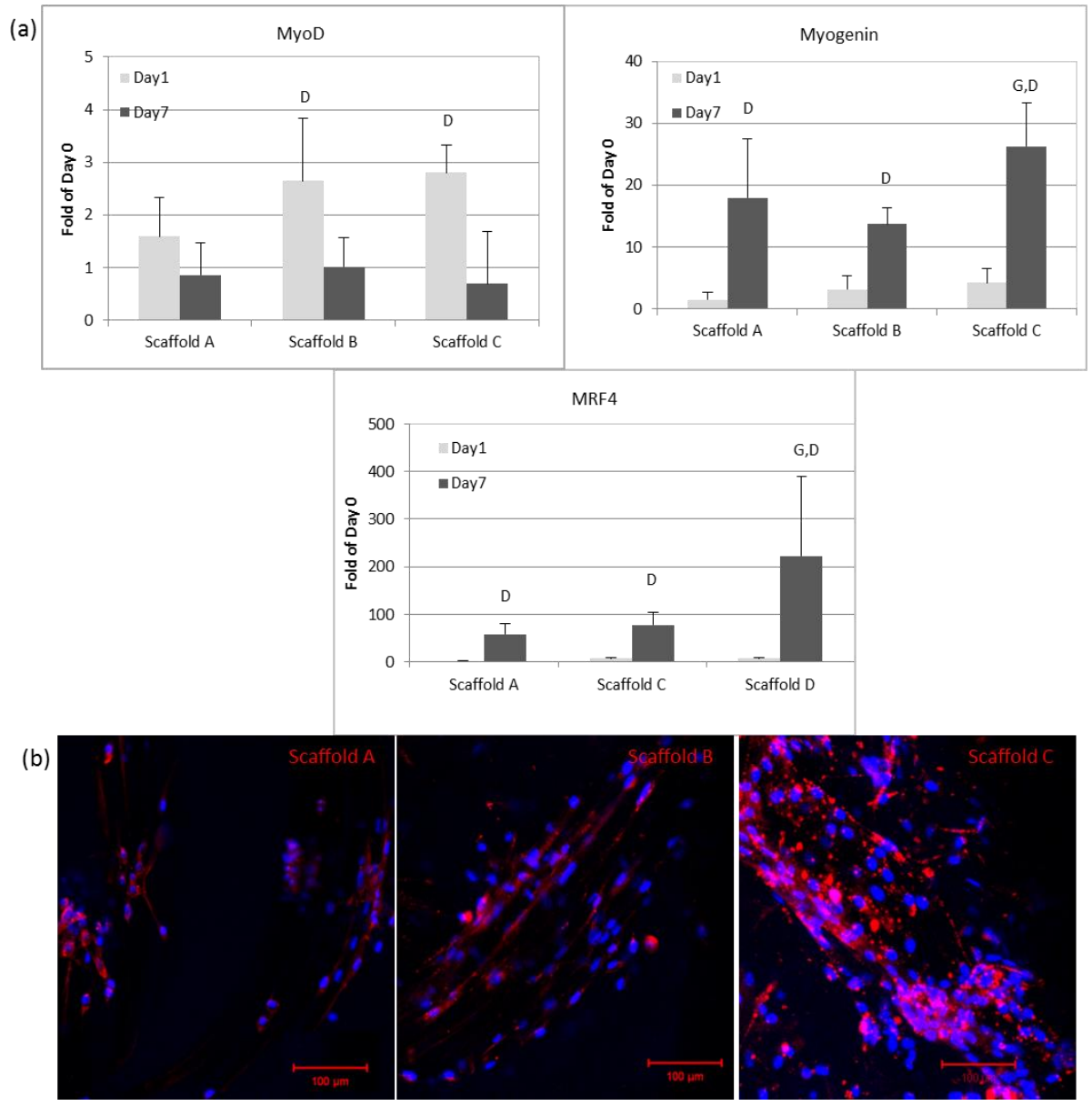
(a)
MyoD
Day1
Day7
Fold of Day 0
D
D
Scaffold A
Scaffold B
Scaffold C
Myogenin
Day1
Day7
Fold of Day 0
D
D
G,D
Scaffold A
Scaffold B
Scaffold C
MRF4
Day1
Day7
Fold of Day 0
D
D
G,D
Scaffold A
Scaffold C
Scaffold D
(b)
Scaffold A
Scaffold B
Scaffold C
100 µm
100 µm